# A Molecular Modeling Study of Entropic and Energetic Selectivities in Air Separation with Glassy Polymers

**Premkumar S. Rallabandi,[†] Aidan P. Thompson,[‡] and David M. Ford*[,†]**

*Department of Chemical Engineering, Texas A&M University, College Station, Texas 77843-3122; and Computational Biology & Materials Technology Department, Sandia National Laboratories, Albuquerque, New Mexico 87185-1111*

*Received September 21, 1999; Revised Manuscript Received January 14, 2000*

ABSTRACT: Air separation is challenging due to the similarities in the sizes and energetics of oxygen and nitrogen. Although polymer membrane-based technology has achieved some success in replacing conventional air separation methods, the effectiveness of polymers has been shown to fall short of the economically attractive region occupied by inorganic microporous materials. Koros and co-workers have recently proposed that this lack of performance is a manifestation of the low entropic selectivity in polymers, possibly due to chain mobility or free volume effects. In this work, we address the effects of chain mobility on selectivity using molecular models and transition-state theory. We employ the methodology recently developed by Greenfield and Theodorou (*Macromolecules* **1998**, *31*, 7068) in which the polymer degrees of freedom can be explicitly included in the hopping rate calculations. About 100 oxygen and nitrogen jump events are studied in three different glassy polypropylene configurations. To examine the effects of polymer rigidity, two separate cases are considered for each jump; in the first case, the polymer model is held completely rigid during the event, while in the second the polymer torsional degrees of freedom are allowed to participate. The results show that the effects of polymer flexibility are reflected most significantly in the energy barriers, with the entropy barriers only marginally affected. Whereas the energetic selectivity can be reduced by 4 orders of magnitude in going from the rigid model to the flexible one, the entropic selectivity generally shows little change. The results are discussed in the context of current experimental and theoretical understanding of these systems.

## I. Introduction

Permeation of small molecules in polymers occurs via the "solution−diffusion" mechanism.[1] As the name suggests, in this mode, permeation occurs in two distinct steps: solvation of the penetrant in the polymer matrix and subsequent diffusion of the same through the polymer. Hence the permeability $P$ can be written concisely as $P = DS$, where $D$ is the diffusivity and $S$ is the solubility of the penetrant. In a binary mixture of gases A and B, the selectivity of A with respect to B is given by

$$\alpha_{A/B} = \frac{P_A}{P_B} = \frac{D_A}{D_B}\frac{S_A}{S_B} \quad (1)$$

Both permeability and selectivity are important in evaluating the performance of a material. Whereas the former is equivalent to the throughput of a separation process, the latter measures the effectiveness of separation. Equation 1 clearly shows that selectivity is affected by two separate quantities: diffusivity and solubility. Although these quantities in general are functions of gas composition across the membrane, at low gas loadings such dependencies may be neglected, and $\alpha_{A/B}$ is referred to as the ideal selectivity.

When dealing with mixtures of nonpolar gases of similar sizes, separation based on solubility is not very attractive. In such cases, one instead exploits differences in the diffusivities of the components. To understand the process of penetrant diffusion through glassy polymers, the microstructure in these materials can be pictured as a network of free volume packets. These packets, where the penetrant molecules spend most of their time, are connected by narrow constrictions or "necks." Diffusion occurs as thermal motion of the polymer and/or thermal activation of the penetrant allows crossings through these necks. Hence, the diffusivity of a penetrant depends on the physicochemical properties of the polymer matrix, such as the fractional free volume (determined by the interchain packing) and the stiffness of the polymer backbone (related to the glass transition temperature, $T_g$). An ideal membrane material would be composed of high free volume that facilitates diffusion and tight constrictions that provide effective sieving. Glassy polymers, which possess these favorable characteristics, have been successfully used as membranes in effecting several industrially important separations. Rubbery polymers, on the other hand, give high permeation rates but are poor sieves due to the absence of rigid necks.[2,3]

Much success has been gained by chemically modifying polymers to create better materials for gas separation.[2,3] However, the performance of diffusion-selective polymers has been observed to be limited by an inverse relationship between permeability and selectivity. Conceptually, this occurs because the magnitudes of the diffusion barriers are generally increased when enhancing the selectivity. Robeson[4] carried out an extensive survey of the performance of polymeric membranes in separating several pairs of gases, clearly demonstrating this permeability-selectivity tradeoff. Singh and Koros[5] further analyzed Robeson's data to point out that the performance of the available polymeric membranes falls short of the economically attractive region currently occupied by zeolites and molecular sieves.

* Corresponding author. Telephone (409) 862-4850. Fax: (409) 845-6446. E-mail: d-ford@chennov2.tamu.edu.
[†] Texas A&M University.
[‡] Sandia National Laboratories.

10.1021/ma991599u CCC: $19.00 
Published on Web 03/31/2000

Singh and Koros[5] reasoned that this difference in performance between polymers and inorganic molecular sieves is caused by the superior entropic selectivity offered by the latter materials. Using transition-state theory (TST), the ratio of diffusivities of species A and B in a gas mixture can be written as

$$\frac{D_A}{D_B} = \exp\left(\frac{\Delta S_{A,B}}{k_B}\right) \exp\left(-\frac{\Delta U_{A,B}}{k_B T}\right) \tag{2}$$

where $k_B$ is the Boltzmann constant, $T$ is the temperature, and $\Delta S_{A,B}$ and $\Delta U_{A,B}$ are, respectively, the differences in entropy and energy barriers encountered by species A and B

$$\Delta S_{A,B} = \Delta S_A - \Delta S_B \tag{3a}$$

$$\Delta U_{A,B} = \Delta U_A - \Delta U_B \tag{3b}$$

Loosely speaking, the activation entropy for a jump event is a measure of the difference in confinement of the molecule between the transition state and the minimum. The first exponential term on the right-hand side of eq 2 is the entropic selectivity, while the second exponential term is the energetic selectivity. By correlating experimentally measured $O_2/N_2$ separation data using eq 2, Singh and Koros concluded that whereas 4A zeolite and carbon molecular sieves offer significant entropic as well as energetic selectivities, even the best current polymers (e.g., polypyrrolone) offer entropic selectivities close to unity.

Singh and Koros[5] hypothesized that this loss in entropic selectivity is consistent with the picture of a penetrant being relatively "unconfined" by a sieving neck in a polymer, due to the relatively large thermal motion of the polymer chains. That is, the local structure of the polymer will relax during a penetrant hopping event, allowing the penetrant significant rotational freedom in the transition state. Zimmerman and Koros[6] subsequently presented several other possible molecular-level scenarios, based on free volume arguments, that would lead to a lack of entropic selectivity. They pointed out that situations where the penetrants are tightly confined in the *minima* might be expected in polymers and that this would tend to decrease the entropic barriers for the individual penetrants as well as the entropic selectivity.

The reason for the relatively small entropic selectivities of polymers is still a matter of speculation, especially with regard to the relative contributions of free volume and inherent molecular-level flexibility. The main aim of this paper is to begin using molecular-level modeling to address these issues, by studying the effects of matrix flexibility on the entropic and energetic selectivities in model glassy polymers. Such analysis will yield valuable information regarding the significant factors that contribute to the performance of polymer membranes. This in turn could provide new directions in research aimed at design of better polymers with superior separation capabilities.

Molecular modeling, and molecular dynamics simulation in particular, have developed into useful tools for probing penetrant diffusion in polymers.[7] Because of the time scale limitations of molecular dynamics, several groups have recently developed alternative theoretical approaches based on combinations of TST and molecular models;[8−12] these approaches have allowed time scales on the order of mircoseconds, and even milliseconds, to be accessed. Gusev and co-workers used TST to study gas diffusion in polymer models which were perfectly rigid[8] and which included mean-field thermal motion;[9] inclusion of the thermal motion of the polymer atoms was seen to have a significant impact on the calculated diffusion coefficients. Greenfield and Theodorou[11,12] devised a novel way to directly include the polymer degrees of freedom (dof's) that contribute to the diffusive jump of a penetrant in the TST formalism. Using this methodology, a number of hopping events of a spherical methane molecule in glassy atactic polypropylene (aPP) were studied, and rates of hopping were calculated by making a harmonic approximation in all relevant degrees of freedom. In this work, we used their method to study the entropic selectivity offered by aPP in the sieving of $O_2$ and $N_2$, but our penetrants are modeled as rigid dumbbells with their rotational degrees of freedom explicitly included, as opposed to idealized spheres.

A brief discussion of the transition-state theory formulation of Greenfield and Theodorou[12] is presented in the next section. Details of the model systems are given in section III. The calculation details are described in section IV. Section V discusses the results of the present study, and conclusions are given in section VI.

## II. Transition-State Theory

Transition-state theory addresses the rate of occurrence of rare events, such as penetrant diffusion in glassy polymers, where adjacent sorption sites are separated by energy barriers much greater than the thermal energy.[13−15] These events happen on time scales that are beyond the range amenable to study by conventional molecular dynamics simulations. For an activated process, the rate of occurrence can be written as[16,17]

$$k^{TST} = \frac{k_B T}{h}\frac{Q^{\ddagger}}{Q^0} = \frac{k_B T}{h}\exp(-\beta \Delta A) \tag{4}$$

where $k^{TST}$ is the rate constant (with units of inverse time), $Q$ is the partition function, $\Delta A$ is the free energy barrier, $\beta = 1/k_B T$, and $h$ is the Planck constant. The superscripts ‡ and 0 indicate the transition state and the minimum, respectively. Using the definition of Helmholtz free energy, this equation can be used to derive the selectivity equation, eq 2.

Previous molecular dynamics studies have revealed the involvement of the torsional motion of chains in the hopping motion of the penetrant during diffusion in polymers.[18] Hence it is important to incorporate the polymer dof's in the search for transition states and the subsequent evaluation of the partition functions and the rate constants. As mentioned above, Greenfield and Theodorou[11,12] studied a number of hopping events of a (spherical) methane molecule in atomic-level models of glassy polymer structures. The authors developed an efficient technique to incorporate polymer degrees of freedom, such as torsional motions and bond angle vibrations, in a self-consistent manner when describing the motion of the penetrant during diffusion. The authors also derived an expression for the rate of hopping within the harmonic approximation; the potential energy of the system was treated as a simple harmonic function in all dof's, including those of the participating polymer segments, in the transition state

and the minimum.[19] Due care was taken to ensure that the end result was independent of the coordinate system used. Using the quantum mechanical vibrational partition function, the resulting rate expression for a hop involving a total of $n$ dof's was given by

$$k^{\mathrm{TST}} = k_0 \exp(-\beta \Delta U) \tag{5a}$$

where

$$k_0 = \frac{k_B T}{h} \frac{\prod_{i=1}^{n} \left[1 - \exp\left(\frac{-h\nu_i^0}{k_B T}\right)\right]}{\prod_{i=2}^{n} \left[1 - \exp\left(\frac{-h\nu_i^{\ddagger}}{k_B T}\right)\right]} \tag{5b}$$

and

$$\Delta U = (U^{\ddagger} - U^0) \tag{5c}$$

with $\nu_i^0$ the vibration frequency of mode $i$ in the minimum and $\nu_i^{\ddagger}$ the vibration frequency of mode $i$ in the transition state. Note that in the denominator of eq 5b, $i = 1$ corresponds to the diffusion direction (along which the vibration frequency is imaginary), so this term is not included in the product. The entropy barrier $\Delta S$ can be calculated using the relation[12]

$$\Delta S/k_B = \ln\left(\frac{h k_0}{k_B T}\right) - 1 \tag{6}$$

Given a jump event of a penetrant from one minimum energy position to another through a transition state, the energy and entropy barriers can be determined from eqs 5c, 5b, and 6, and the total rate for that jump event can be obtained from eq 5a.

The approach taken in this paper will be to consider individual jump events, calculate the energetic and entropic barriers for each penetrant ($O_2$ and $N_2$) separately, and then use eq 3 to estimate an entropic and an energetic selectivity for each jump. Since the macroscopic selectivity is ultimately determined by the selectivities of individual hopping events, our results will provide insight on macroscopic behavior. However, note that we do not actually predict a ratio of macroscopic diffusion coefficients. Such macroscopic properties could be estimated, but significantly more effort and statistical analysis is necessary; this will be the subject of future work.

To proceed with our analysis of transport in a polymer, we must first prescribe an atomic-level model of a polymer/penetrant system, including interaction potentials. Then we must locate transition states and associated minima to define hopping events, and evaluate rate constants based on the information at the transition states and minima.

## III. Model and Potential Details

**A. Polymer and Penetrant Models.** The atactic polypropylene (aPP) models used in this study were very similar to those used by Greenfield and Theodorou.[11,12] These structures were parametrized in terms of the various bond lengths, Eulerian, bond, and torsional angles, and chain-start positions following Theodorou and Suter.[20] We review only the most important features here; the interested reader is referred to their publications for details. We employed polymer structures with three polymer chains of 50 monomers each at a density of 0.892 g/cm$^3$; this is equal to the experimental density at 233 K, which is ca. 20 K below the $T_g$ of aPP.[20] The polymer model, which was cubic and periodic in all three dimensions, had a side length of 22.79 Å. The repeat unit of the polymer is depicted in Figure 1; we followed the previous authors[11,12,20] in using the "united atom" model for the methyl units and explicit atom models for the rest of the species. The C−C and C−H bond lengths are constrained at their mean values. Whereas Greenfield and Theodorou[11,12] considered the bond-angles to be flexible, we considered them also to be constrained at their mean values to reduce the computational requirement. A molecular dynamics study by van Gunsteren and Karplus[21] demonstrated that the assumption of rigid bond angles can affect the dynamics of complex model molecules, damping positional fluctuations and dihedral angle transition rates relative to those in unconstrained models. Our flexible polymer model will therefore be somewhat less flexible than that of Greenfield and Theodorou,[11,12] but we expect that our comparative study of flexible and perfectly rigid polymers will not be qualitatively affected by this assumption.

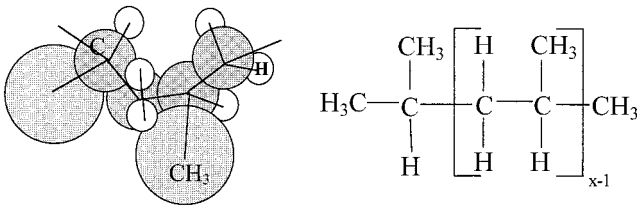


| Bond lengths (Å) | | Bond angle supplements (degrees) | |
|---|---|---|---|
| C-C | 1.53 | intradyad C-C-C | 66.0 |
| C-H | 1.10 | interdyad C-C-C | 68.0 |
| C-$CH_3$ | 1.53 | intradyad C-C-H | 71.0 |
| | | interdyad C-C-$CH_3$ | 68.0 |
| | | interdyad C-C-H | 73.2 |

**Figure 1.** Chemical structure of atactic polypropylene. The bond lengths and angles were constrained, during all calculations, at the values shown here.

The initial polymer structures were generated at the given density and temperature using the Polymer Builder module of the CERIUS$^2$ software from Molecular Simulations Inc.[22] This module samples the torsional angles using the RIS method[23] while avoiding significant overlaps between polymer atoms.[20] After the polymer structure was built, the Energy Minimizer module of the software was used to obtain a preliminary glassy matrix. The AMBER force-field was employed during this step, with the bond-length and angle-bending spring constants modified to very high values; this led to a minimized structure with bond lengths and angles essentially fixed at the desired values. The final glassy polymer structure was created by further minimizing the potential energy in terms of only the torsional angles, chain start positions, and Eulerian angles.[24] The BFGS algorithm, as implemented in FORTRAN by Byrd et al.,[25] was used for this purpose; no penetrants were present in the polymer matrix during energy minimization. The penetrant jump re-

**Table 1. Pure Component LJ Parameters**

| species | $\sigma$ (Å) | $\epsilon$ (kcal/mol) | reference |
|---|---|---|---|
| $CH_3$ | 3.564 | 0.1388 | Greenfield and Theodorou[11] |
| C | 3.207 | 0.0841 | Greenfield and Theodorou[11] |
| H | 2.316 | 0.0763 | Greenfield and Theodorou[11] |
| N | 3.310 | 0.0741 | Fischer and Lago[51] |
| O | 3.090 | 0.0886 | Fischer and Lago[51] |

sults presented here were obtained from studies carried out in three independently built glassy polymer structures.

The diatomic penetrant molecules, $O_2$ and $N_2$, were modeled as rigid dumbbells with the two force centers separated by a distance equal to the equilibrium bond-length (1.0166 and 1.0897 Å respectively). Unlike spherical molecules, these penetrants have five degrees of freedom: the three Cartesian coordinates of its center of mass and two Eulerian angles.[24]

**B. Potentials.** The total energy of the penetrant−polymer system is given by

$$U = U_{\text{tor}} + U_{\text{poly-poly}} + U_{\text{poly-pen}} \tag{7}$$

where $U_{\text{tor}}$ is the torsional energy associated with the rotation of the skeletal bonds, $U_{\text{poly-poly}}$ is a pairwise sum of the nonbonded interactions between the polymer segments, and $U_{\text{poly-pen}}$ is the corresponding quantity evaluated between polymer segments and the two force centers on the penetrant. The potential energy expressions and most of the parameters employed therein were taken from Theodorou and Suter;[20] these are briefly described below.

The torsional energy is given by

$$U_{\text{tor}}(\phi) = \frac{k_\phi}{2}(1 - \cos 3\phi) \tag{8}$$

where $\phi$ is the torsional angle. A value of 2.8 kcal/mol was used for $k_\phi$.

The polymer−polymer and polymer−penetrant nonbonded interactions were modeled with the site−site 12−6 Lennard−Jones (LJ) potential. To ensure that the energy function and its first and second derivatives were continuous in the entire range of the center-to-center distance $r$ between two species, the attractive tail of the potential was approximated by a quintic spline.[20] The expression of the potential is given in Appendix A. The pure component LJ parameters for the different species are given in Table 1. The LJ parameters for cross-interactions were calculated from the pure component values using Lorentz−Berthelot mixing rules.[26] Periodic boundary conditions with the usual minimum image convention[26] were employed to eliminate surface effects.

## IV. Details of Calculation

**A. Geometric Analysis of Polymer Structures.** The first step in studying the hopping motion of a penetrant is the location of the transition state, i.e., the lowest-energy point on the (hyper) surface that separates the "reactant" and the "product" states. In general, the transition state is physically located in the vicinity of the neck that separates two adjacent packets of free volume present in a microporous material, such as a polymer. In a material made of atoms arranged in a relatively simple geometrical pattern, e.g., in a zeolite with well-defined cages and sieving windows arranged on a regular lattice, the transition states can be located in a straightforward way. In a polymer model, on the other hand, the energy landscape is very complex and hence the location of the transition states is not trivial. This task becomes even more difficult when the polymer dof's are considered as flexible, i.e. when the polymer structure is allowed to rearrange in response to the presence of the penetrant. Hence the location of transition states in a flexible polymer model requires the use of sophisticated search techniques. The success of these algorithms in yielding a viable transition state depends on the proximity of the initial guess configuration to that in the transition state.

Since the physical "terrain" in a polymer matrix does correspond to the energy landscape (e.g., constrictions roughly correspond to the energy maxima), geometric analysis of the polymer structures is useful. Several researcers have employed Delaunay tessellation[27,28] or fine grid maps[29] to visualize the free volume clusters accessible to hard-sphere probes of different diameters, and to locate possible constrictions bridging two adjacent cavities.

In this work, we used a more direct methodology of surveying the polymer−penetrant interaction energy in the polymer models to accomplish this task. Since the penetrant position in a transition state in the rigid model correlates well with that in the corresponding flexible case, we used the rigid models to generate several initial guesses for the transition state search. Although true diatomic penetrants were eventually used in this study, a monatomic penetrant was used in the geometric analysis. Hence there are only three degrees of freedom in the problem, which greatly simplifies the energy sampling to study the microstructure of the polymer models. The basic approach, presented below, is similar to that used by Gusev and Suter[30] and June et al.[31]

The three-dimensional configurational space was discretized as a cubic grid of volume elements or voxels, with grid-spacing $a$. In our study, the energy of interaction $U_{\text{poly-pen}}$ between the polymer and a penetrant particle located at the center of each voxel was calculated. Voxels with energies beyond a cutoff value of $75k_BT$, which signifies significant overlap with the polymer excluded volume, were dropped from the subsequent analysis. For each voxel, the lowest energy was determined from the 27 values occurring in the $3 \times 3 \times 3$ cube centered on the current voxel. If the central voxel has the lowest energy, then this point is a local minimum. Ties were resolved by always choosing the voxel which occurs later in the arbitrary ordering of the voxels by position.

Once this has been done, it is computationally inexpensive to partition the voxels into a set of cavities which cover the entire three-dimensional volume of the polymer. To understand this, it is helpful to imagine an arrow drawn from each voxel to its minimum energy neighbor. According to the procedure described above, a voxel can have zero, one, two, or more arrows entering it, but only one arrow leaving it (or zero if it is a minimum). These properties result in the arrows forming a set of arborescences, which are directed graphs with no loops and only one root. Hence there is a one-to-one correspondence between cavities and root voxels. In addition, all points belonging to a given cavity can be found by starting at the root voxel, and finding all the voxels which are connected to it. Computationally, this was done by identifying which of the 26 neighbors

of the root voxel had it as their minimum energy neighbor. These voxels belong to the same cavity as the root voxel. Their neighbors were checked in turn, and the process was repeated in an iterative fashion until no more members of the current cavity were found. By repeating this for all the root voxels, every voxel is attributed to one and only one cavity.

Once the voxels were partitioned into cavities, we proceeded to evaluate properties of the cavities, and the dividing surfaces between cavities. For example, the physical volume $V_i$ of cavity $i$ is simply the number of voxels in the cavity, multiplied by $a^3$. The partition function $Q_i$ of cavity $i$, which is the integral of the Boltzmann factor $\exp(-U_{\text{poly-pen}}/k_BT)$ over the cavity volume, can be computed by summing the Boltzmann factors calculated for each voxel.

To find transition states, the boundaries or dividing surfaces between cavities must be located. We defined cavity boundaries by boundary voxels, for which one or more of the six nearest neighbors belongs to a different cavity. The location of the transition state was taken to be the center of the minimum energy boundary voxel. The coordinates of the transition states identified in this manner were used as initial guesses in the subsequent saddle point searches in rigid and flexible polymer models using a dimer penetrant.

**B. Methods for Location of Transition States and Minima.** In the transition state (TS), which is a first-order saddle point, all but one of the normal modes (which corresponds to the diffusion direction) have real frequencies. Hence the Hessian (the matrix of second derivatives of total potential energy) evaluated at the TS has a single negative eigenvalue. The work of Cerjan and Miller[32] provides the basis for most techniques employed in the literature for saddle point searches. Baker[33] summarized the original work along with the later developments and made an algorithmic presentation of the technique, which is popular among researchers. Greenfield and Theodorou[11,12] also employed Baker's algorithm[33] in their work. Wales[34,35] followed a slightly different approach in formulating the optimization problem. Whereas two different shift parameters, referred to as $\lambda_p$ and $\lambda_n$, are used for the maximizing and minimizing modes in Baker's algorithm,[33] Wales introduced separate shift factors along all normal modes; a larger variety of high-dimensional problems could be solved more effectively using Wales' algorithm. In the present work, which involves systems with anywhere from 100 to 200 total dof's, Wales' algorithm was also generally found to be more efficient. We caution the readers here that this statement is not intended to be a general prescription since no systematic and thorough comparison of the performance of the two methods was carried out.

Once a TS is located, the corresponding minima were located by following Fukui's intrinsic reaction coordinate (IRC) methodology.[36] Banerjee and Adams[37] appropriately modified the original prescription to make it consistent with the use of generalized coordinates ($\mathbf{q}$), as opposed to mass weighted Cartesian coordinates. As mentioned earlier, the generalized coordinates include the five penetrant dof's, the polymer torsional and Eulerian angles, and chain start positions. The reaction path involving generalized coordinates is described by the following prescription[12] for a step $d\mathbf{q}$

$$\mathbf{a}^0\, d\mathbf{q} = \nabla_{\mathbf{q}} U\, d\tau \tag{9}$$

where $\mathbf{a}^0$ is the covariant metric tensor calculated based on the flexible dof's and $d\tau$ is a scaling factor used to adjust the step size. The size of the multidimensional step, $ds$, was calculated by the equation[12]

$$ds^2 = (d\mathbf{q})^T\, \mathbf{a}^0 (d\mathbf{q}) \tag{10}$$

Since the gradient of potential energy with respect to all flexible dof's is zero in the TS, the first step from the TS must be treated differently than prescribed in eq 9. Generally the pathways to each of the minima were initiated along the eigenvector corresponding to the single negative eigenvalue of the following generalized eigenvalue problem[12,37]

$$(\mathbf{H}_{qq} - \lambda\, \mathbf{a}^0) d\mathbf{q} = \mathbf{0} \tag{11}$$

where $\mathbf{H}_{qq}$ is the Hessian with the derivatives evaluated with respect to the flexible degrees of freedom and $\lambda$ are the eigenvalues.

**C. Implementation of Rate Calculations. Rigid Polymer.** Each search for a transition state was initiated by inserting a single penetrant molecule into the energy-minimized polymer structure. The center of mass of the diatomic gas molecule was first placed at the coordinates of a TS located by the geometric analysis detailed above; the orientation of the penetrant was chosen randomly. Since the penetrant used in the geometric analysis was a spherical oxygen molecule, as opposed to a dumbbell model used in the rest of the steps, a new transition state in penetrant dof's was found using Wales' algorithm. The two minima associated with this TS were located by following the IRC prescription discussed earlier; a step size $ds$ of 0.001 $(g/mol)^{1/2}$ Å (calculated using eq 10) was used in calculating the diffusion path. Finally the rates of hopping in both directions were evaluated using eq 5, with the frequencies calculated from the eigenvalues of the Hessian matrix at the appropriate locations.

**Flexible Polymer.** The presence of a penetrant naturally perturbs the polymer structure in its immediate vicinity, and the polymer degrees of freedom, such as torsional motions, in turn affect the hopping process of the gas molecule. Hence determining which of the polymer dof's are to be treated as flexible is important for obtaining an accurate estimate of the hopping rate. As pointed out by Greenfield,[38] too many polymer dof's cannot be treated as flexible due to the constraints on computational power and, more importantly, to avoid studying the effects of long-range chain rearrangements as opposed to the more relevant, local segmental motions. On the other hand, one might expect that at least those polymer segments which enter the potential range of the penetrant during a hop event should be treated as flexible. Following Greenfield and Theodorou,[12] when segment $i$ along the chain is found within the potential cutoff from the penetrant, the nearest six torsional angles are treated as flexible. If that segment happens to be a chain start, its position as well as the Eulerian angles were also treated as flexible.

Since the penetrant travels significant distances in the course of a hop, it is important to include the polymer dof's along the diffusion path. Greenfield and Theodorou[12] addressed this issue by including additional dof's in the IRC calculation whenever a new polymer segment was found within the penetrant's sphere of interaction. We believe that it is more desirable to make an a priori estimate of all of the dof's along the path

that need to be treated as flexible and find the transition state in all of these relevant dof's. Our initial estimate for the relevant degrees of freedom is obtained from the hopping event in the rigid polymer model. At the transition state in the rigid polymer, we note all polymer segments that are within the potential cutoff from the two penetrant centers. Subsequently as the penetrant moves along the diffusion path during the rigid−polymer IRC calculation, this list is augmented with the new polymer segments encountered by the penetrant. All degrees of freedom associated with the final list of atoms, after locating the two minima, are treated as flexible in studying the corresponding hop in flexible polymer model.

Next we discuss the actual search for the transition state in this high-dimensional space. Starting with the T*S* configuration in the rigid polymer and a list of dof's from the rigid case, a higher dimensional transition state in the penetrant and polymer dof's was found by "releasing" the latter set in an incremental fashion. This procedure is similar to the one suggested by Greenfield and Theodorou,[12] who found that the TS search is much quicker when polymer dof's are included in steps than when all were treated as flexible simultaneously. We first picked the five polymer segments closest to each of the centers of the penetrant dumbbell and treated all the torsional angles associated with them as flexible. After the higher dimensional transition state was found, the dimensionality of the problem was further increased by releasing more polymer dof's. This process was continued until we treat as flexible all the torsional angles associated with the polymer segments found within the potential cutoff distance from the penetrant. After this, we also released all the dof's in the list compiled earlier along the IRC path in the rigid polymer and found the corresponding transition state. Subsequently, the IRC following was initiated, and the two minima were found. As before the rates of hopping were found using eq 5. Interestingly, the inclusion of additional degrees of freedom in the calculation (beyond those relevant at the transition state) did not significantly alter the energy and entropy barriers and selectivities.

As a consistency check, a list of dof's that should be treated as flexible was compiled along the high-dimensional IRC path in the flexible polymer, and it was compared with the original list based on the rigid polymer. In most cases, fewer than six new torsional angles were added to the list, which on average corresponds to one more polymer segment being treated as flexible. We found that including these new dof's further in the transition state search and IRC path evaluation did not alter the rate constant values significantly; hence they were not included in obtaining the results reported here. For those cases where many more new polymer dof's were added (about 15% of the total), the spatial locations of the transition state and/or minima were observed to change substantially (>2 Å) relative to the positions in the rigid case. This indicated that the character and path of the hop had changed significantly upon introducing polymer degrees of freedom. There is nothing physically unrealistic about such a result, so these hops were included in the calculation of aggregate statistics such as median energy and entropy barriers. However, since these hops are no longer correlated with the original hop in the rigid polymer, we chose not to include them when the rigid and flexible polymer models were directly contrasted. Since the nitrogen molecule is larger than the oxygen molecule, more polymer dof's are treated as flexible during its hop. The TS configuration found for the latter is used as the initial guess for the former to save computer time.

We studied several hops of the penetrants starting with different initial guesses for the penetrant placement in three independent glassy polymer structures. In almost all cases the negative eigenvalue occurred in one of the penetrant degrees of freedom; similar behavior was also observed by Greenfield.[38] In some instances, the transition state search in the rigid polymer yielded configurations in which the negative eigenvalue was seen along one of the Eulerian angles of the penetrant. These jumps were observed to be not diffusive but rather related to molecular rotation; the jump length in such cases was virtually zero. Hence, we present here only those results where the negative eigenvalue occurs in one of the Cartesian directions of the penetrant. In all, 42 distinct hopping events were studied. Since each jump has two rate constants (forward and reverse) associated with it, we have 84 rate constants.

## V. Results and Discussion

**A. Results. Energy and Entropy Barriers in Rigid Polymer Models.** The energy and entropy barriers for oxygen in rigid polymer models are plotted against the hopping distance $d$ (i.e. displacement of the penetrant center of mass from the transition state to the minimum, which is different from the "path length" of the hop) in Figures 2a and b, respectively. As can be seen from the plots both barriers take on a range of values: $\sim 0.01$ to $\sim 10 k_B T$ in the case of $\Delta U$ and $1-10 k_B$ in the case of $\Delta S$. The distance $d$ ranges from near 0 to 7.5 Å; this wide range of values signifies the heterogeneity of the local microstructural features within the polymer matrix. We would like to point out that the entropy barriers are negative because the penetrant is more constrained and hence has lower entropy in the transition state compared to when it is in the minimum. Similar ranges of activation barriers were seen by Greenfield and Theodorou[12] during the hopping of a spherical methane molecule.

On the basis of the free energy values of the two minima, each of the two rates in a given jump event can be assigned a direction. By analogy with chemical kinetics, the "forward" event is defined as movement from the minimum of higher free energy to that of lower free energy, and the "reverse" event is of course defined as the opposite. A significant correlation between the direction of motion and the magnitude of the energy barrier might be expected, but none was detected in this work; the "forward" and "reverse" rate data were well-mixed in plots such as Figure 2 (not explicitly shown).

We can see from parts a and b of Figure 2 that both $\Delta U$ and $-\Delta S$ are positively correlated with distance $d$. Interestingly, the energy and entropy barriers exhibit different behaviors above and below a $d$ of $\sim 2$ Å. Typically, $\Delta U$'s below this hop distance are less than or close to $k_B T$. Hence the corresponding hops are not activated. Entropy barriers also behave differently above and below a $d$ of 2 Å. For $d < 2$ Å, $\Delta S$ values do not show much scatter, but tend to be in a narrow range between $-2$ and $-4 k_B$. On the basis of the small distances, these jumps likely occur within the sorption site; they are so-called "intramacrostate" hops that do

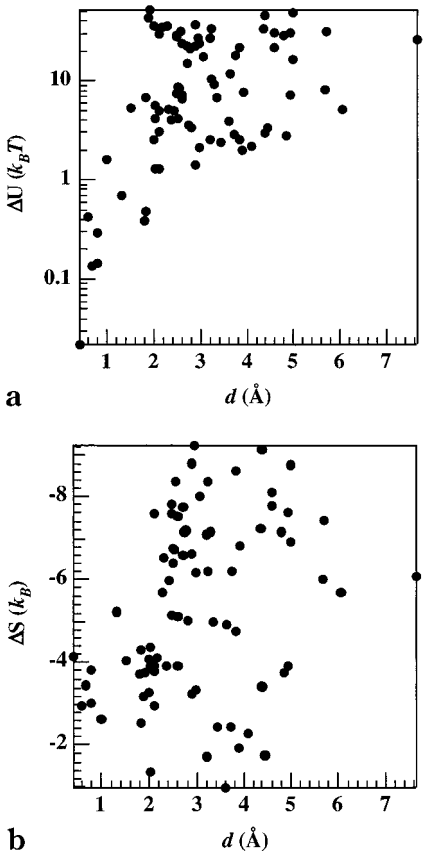


**Figure 2.** Energy barriers (a) and entropy barriers (b) during oxygen hopping in the rigid polymer models. *d* is the distance from the location of the transition state to the associated energy minimum.

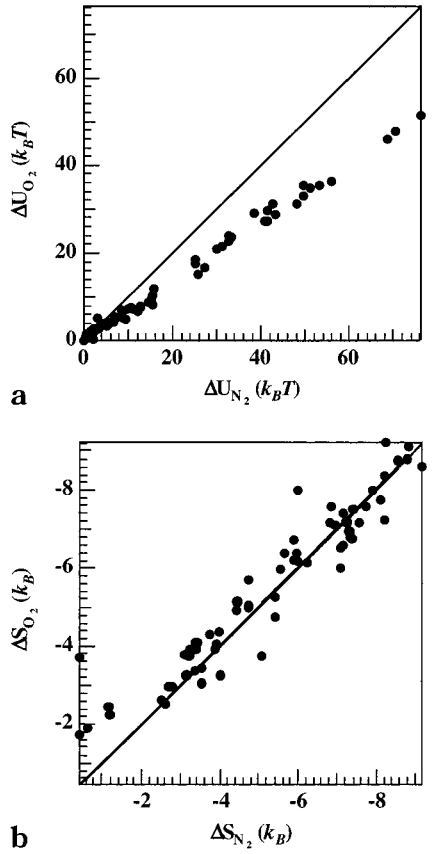


**Figure 3.** Comparison of energy barriers (a) and entropy barriers (b) for oxygen with those for nitrogen in the rigid polymer models.

not contribute to the overall diffusion of the penetrant.[12] The hops with $d > 2$ Å are likely the "intermacrostate" jumps that take the penetrant from one sorption site to an adjacent one.

A similar range of values for barriers and hopping distances were seen for nitrogen. The $\Delta U$ values for oxygen are plotted versus those for nitrogen in Figure 3a; a corresponding plot of $\Delta S$ values is given in Figure 3b. By comparing the data against the $y = x$ lines given on the plots, one can see that whereas $\Delta U$ values for $O_2$ are in general lower than those for $N_2$, no such trend is obvious in the case of $\Delta S$. The former observation can be explained based on the sizes of the penetrants: since nitrogen is larger than oxygen, it overlaps more with the polymer atoms comprising the neck, thus possessing the higher potential energy in the transition state. In the cavity, depending on the local packing of polymer segments, nitrogen may have higher or lower energy compared to oxygen. Since the difference in penetrant energies in the minimum is expected to be much smaller than that in the transition state, the energy barrier itself is higher for nitrogen than oxygen.

On the basis of the sizes of the penetrants, one would expect that nitrogen would also have a higher entropy barrier. Judging from the magnitudes of the normal-mode frequencies, nitrogen is indeed more constrained (i.e., has lower entropy) in the transition state compared to oxygen. However, our data indicated that nitrogen is often more constrained compared to oxygen in the *minimum* as well, leading to a decrease in the overall entropic selectivity for the hopping event. Further discussion of this phenomenon and its consequences for the selectivity behavior will be given below.

**Energy and Entropy Barriers in Flexible Polymer Models.** Flexibility of the polymer matrix is expected to lower the energy barriers, since the polymer segments can rearrange to reduce overlaps with the penetrant. The same effect is expected in the case of entropy barriers, since the penetrant presumably is trapped less tightly in a flexible polymer compared to a rigid one. The energy barrier values for oxygen in the flexible polymer are plotted against those in the rigid models in Figure 4a; the corresponding plot of entropy barriers is shown in Figure 4b.

As expected, these plots show that both activation energies and activation entropies decrease as a result of polymer flexibility; however, the effect is seen to be more pronounced in the case of energies, where order of magnitude differences can be seen. Interestingly, when the energy barriers are relatively low ($<\sim 3\ k_BT$), the values in flexible and rigid models seem to be equal to each other. In the case of entropy barriers, similar behavior tends to occur when $\Delta S$ is in the range between $-2$ and $-4\ k_B$. This is probably another indication that the these jumps are happening within a macrostate.

**Rates of Hopping.** Now we shall consider the rate constants calculated for various hops in this study. Parts a and b of Figure 5 show the hopping rates $k^{TST}$ plotted against *d* for oxygen and nitrogen respectively; values in both rigid and flexible models are shown in these plots. We can see that $k^{TST}$ values are spread over a wide range; this is a direct consequence of the wide spread in the energy and entropic barriers seen earlier. A similar range of values for rate constants was seen by

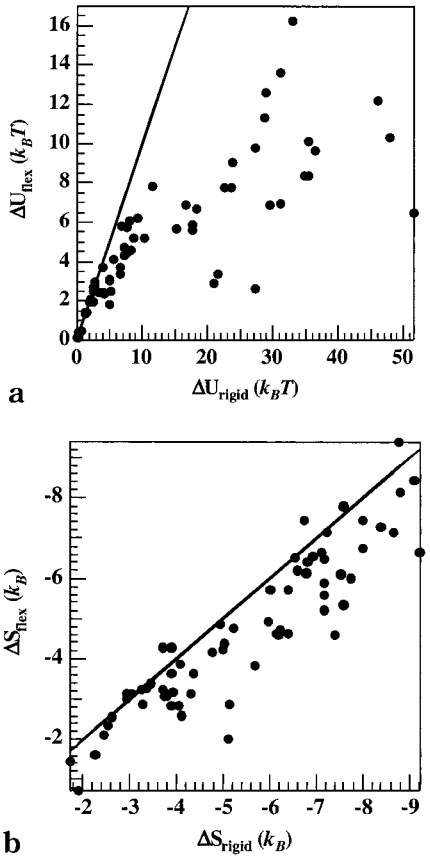


**Figure 4.** Comparison of energy barriers (a) and entropy barriers (b) for oxygen hopping in the flexible models with those in the rigid polymer models.

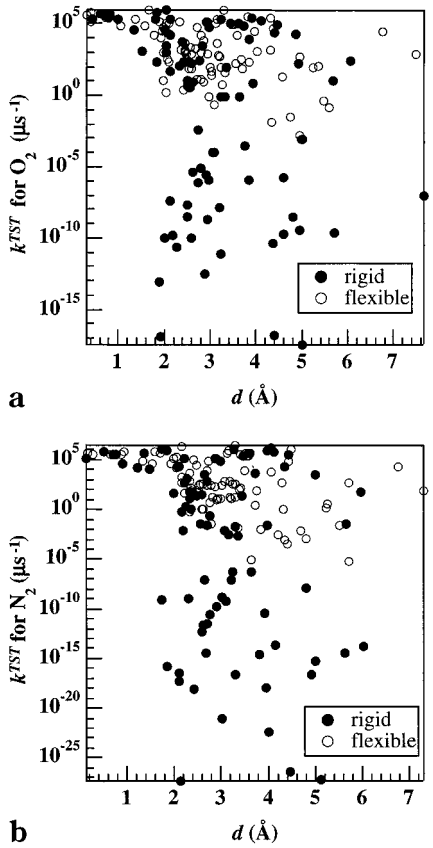


**Figure 5.** Rate constants for oxygen (a) and nitrogen (b) hopping in the rigid and flexible polymer models. *d* is the distance from the location of the transition state to the associated energy minimum.

Greenfield and Theodorou[11,12] for methane in flexible model systems. Since both barriers are lower in the flexible polymer case than in the rigid one, the rates of hopping are generally faster in the former case. We can also see that the nitrogen hops are, in general, slower compared to those of oxygen; this is consistent with the experimental observation that the former species has a lower diffusion coefficient in polymers compared to the latter species.

The behavior of $k^{TST}$ values for $d < 2$ Å requires some discussion. The rate constants in this region have similar values, in the range $10^5-10^6$ $\mu s^{-1}$, for both penetrants; a very similar range of values was seen by Greenfield and Theodorou[12] for the hopping of methane in the course of intramacrostate jumps. This behavior seems to suggest that intramacrostate hops do not closely distinguish between penetrants. Interestingly, hopping rates in this region seem to be unaffected by the flexibility of the polymer matrix.

**Energetic and Entropic Selectivities.** As given in eq 2, selectivity is the exponential of the difference between the corresponding barriers for oxygen and nitrogen. Hence the simple difference between $\Delta U$'s (or $\Delta S$'s) for the two gases is enhanced when converted into the corresponding selectivity. Energetic and entropic selectivities for the different hops are plotted against *d* in parts a and b of Figure 6, respectively. We can see from Figure 6 a that energetic selectivity, in general, is greater than unity; i.e., relative to nitrogen, oxygen encounters smaller potential energy barriers during diffusion. In this plot, we can also see the clear difference in behavior in going from a rigid polymer to a flexible model; evidently, rigidity of the constriction helps to distinguish the two penetrants much more effectively based on potential energy barriers. As the polymer is made locally flexible and capable of responding to the penetrant's presence, the overlaps are decreased, leading to a substantial lowering of the energy barriers, and as a consequence the difference between $\Delta U$'s also decreases. One statistic that illuminates this discussion is the median value of the energy barriers in different situations: the median values of $\Delta U$'s in the rigid polymer models for $O_2$ and $N_2$, respectively, are 7.48 and $12.42k_BT$, whereas the corresponding values in the flexible case are 3.89 and $4.96k_BT$. These findings are consistent with the hypothesis developed by Koros and co-workers[2] that the activation energy for penetrant diffusion should increase with segmental rigidity.

In contrast to energetic selectivity, entropic selectivity (Figure 6b) cannot be said to be always favorable to oxygen relative to nitrogen. Again looking at the median values of entropy barriers for oxygen and nitrogen, in the rigid models the values are $-5.46$ and $-5.47k_B$ respectively, and in flexible models the values are $-4.59$ and $-4.30k_B$, respectively. We can also see from these numbers that rigid and flexible polymer models do not seem to be much different in terms of the entropic selectivity they offer. To look more closely at the effect of flexibility on the two kinds of selectivity, we consider the ratio of the selectivity value in the flexible polymer to the corresponding value in a rigid matrix. Parts a and b of Figure 7, respectively, show energetic and entropic selectivity ratios plotted against *d*. Figure 7a clearly shows that the flexible polymer has a significantly smaller energetic selectivity than the rigid one,

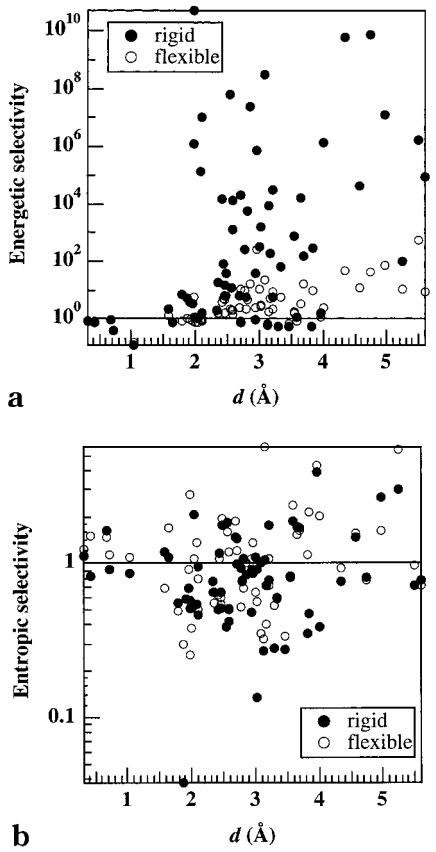


**Figure 6.** Energetic selectivities (a) and entropic selectivities (b) in oxygen/nitrogen separation with the rigid and flexible polymer models. *d* is the distance from the location of the transition state to the associated energy minimum.

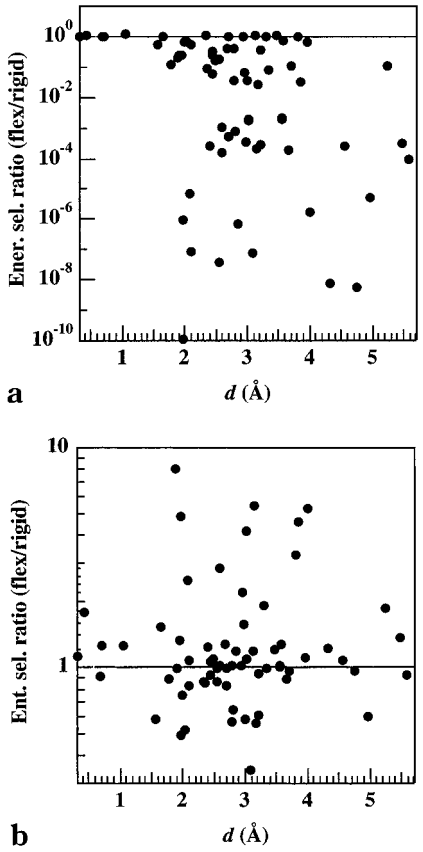


**Figure 7.** Ratios of energetic selectivities (a) and entropic selectivities (b) in the rigid polymer to those in the flexible polymer. *d* is the distance from the location of the transition state to the associated energy minimum.

except for jump lengths smaller than ~2 Å (likely intramacrostate jumps). We believe that this is an indication that polymer dof's do not participate significantly in a intramacrostate jump; similar results were seen by Greenfield and Theodorou.[11,12]

In contrast to the energetic selectivity ratio, Figure 7b shows that the entropic selectivity ratio is never very small, and in fact it is often greater than unity. There is also a great deal of scatter in the data. This would seem to suggest that polymer flexibility does not have a significant effect on entropic selectivity, although the contributions for the individual penetrant species are affected (refer to Figure 4b). There also appears to be some difference in the magnitude of the scatter for the intra- and intermacrostate jumps, with less scatter below $d = 2$ Å.

**B. Discussion.** First we shall summarize the results of the current study. We saw above that a variety of penetrant hopping events is possible in polymers, in which the activation entropies and energies assume a wide range of values. These events are seen to fall into two general categories: ones that occur within a cavity and those that occur across cavities. Both energy and entropy barriers are lower in the former cases, where the minima are located typically within 2 Å from the transition state. Moreover, since polymer degrees of freedom do not seem to participate in these hops, barrier and selectivity values are not affected due to flexibility of the polymer matrix. The intracavity hops do not contribute to the overall diffusion of the penetrant, and hence are relatively unimportant for us. In contrast, the intercavity jumps do contribute to diffusion and will be discussed further below.

For jumps that occur across cavities, where the penetrant passes through a constricting neck to move to an adjacent packet of free volume, the activation barriers are typically higher. Whereas the energetic selectivity is seen to be favorable to oxygen compared to nitrogen, the entropic selectivity fluctuated about unity. The introduction of matrix flexibility substantially lowers the energy barriers and the corresponding selectivities. As mentioned above, this observation is consistent with the hypothesis of a positive correlation between penetrant activation energy and polymer segmental rigidity, as developed in the literature by Koros and co-workers.[2] The entropy barriers for each penetrant are also lowered due to matrix flexibility, although the effect is not as substantial as in the case of energy barriers. However, entropic selectivities are apparently not influenced strongly, or in any particular direction, by flexibility.

The lack of clear effect of polymer flexibility on entropic selectivity is directly at odds with the view of Singh and Koros,[5] who proposed that thermal motion of the polymer chains leads to loss of entropic selectivity in these materials. However, our result is perhaps not very surprising in view of a recent simulation study by Rallabandi and Ford,[39] who calculated diffusivity selectivities for the oxygen/nitrogen separation in model sieving windows. Their approach was based on statistical mechanics and transition-state theory and did not use the harmonic approximation to evaluate the partition functions. Instead, the required free energy differences were directly estimated using a Monte Carlo scheme proposed by Voter.[40] Molecular-level flexibility was included by tethering the solid atoms to their

equilibrium positions with harmonic springs. Simulations were performed at several window widths and flexibilities, i.e., different values of the spring constants (values as low as ~0.01 of the C−C bond strength were used). The results from that study showed that while the energetic part of the total selectivity was quite sensitive to the window flexibility, the change in entropic contribution was never more than about 20%, even for very flexible windows.

As mentioned above, our data indicated that nitrogen is often more constrained than oxygen in the *minimum* as well as in the transition state, leading to a decrease in the overall entropic selectivity for the hopping event. These findings support the hypothesis of Zimmerman and Koros[6] that the small cavity volumes associated with the minima in polymers can have a significant negative impact on entropic selectivity. In particular, our results generally support the picture in Figure 4 of Zimmerman and Koros,[6] where the entropy barrier of nitrogen is lowered due to a high degree of confinement in the minimum. Therefore, we believe that the apparent lack of entropic selectivity in polymers is more likely caused by factors associated with the molecular-level distribution of the free volume, rather than the inherent rigidity of the matrix.

The relatively good entropic selectivity in inorganic materials can also be explained on the basis of free volume.[6] The microstructure of inorganic materials such as zeolites and carbon molecular sieves differs substantially from that of polymers. In the inorganic materials, the structure often consists of wide cages (radius ~6 Å or more) where the motion of small molecules is relatively free, joined by small windows that provide the sieving.[41] In polymers, the distribution of free volume is believed to be much different, although direct experimental determination of free volume distribution in polymers is not a straightforward task. Positron annihilation lifetime spectroscopy (PALS) measurements in polymers revealed that the average hole radius in polymers typically ranges from 2.8 to 3.7 Å.[42] We note that there has been some criticism of the assumptions made in interpreting PALS results,[43] so these reported cavity sizes should be regarded with some caution. Molecular modeling using hard-sphere penetrant probes provides another method for estimating the free volume distribution in polymers.[27−29,44−48] These studies, performed on a range of polymer types, have revealed that the accessible free volume fraction is a sharply decreasing function of probe size and that very little of the unoccupied volume is accessible to probes having radii greater than ca. 2 Å. Of course, larger cavities do exist and can have a significant impact on the overall transport properties. However, based on the results of either PALS or molecular modeling, the typical free volume elements in polymers are expected to be much smaller than the cages seen in the inorganic materials. This scenario may mean that nitrogen tends to be more confined compared to oxygen not only in the sieving neck, but also in the cavity. These differences tend to offset those in the transition state, resulting in an overall decrease in entropic selectivity.

If these conclusions are accurate, materials design efforts for increasing entropic selectivity in polymers should not be targeted toward increasing rigidity per se, but rather toward manipulating the free volume. The ideal would be to create structures similar to those of inorganic molecular sieves, with cavities which are large enough to allow free movement (rotation) of the penetrants. This idea has been considered before.[3] In fact, Zhang[49] synthesized isotactic polyphenyl silsequioxane, a polymer containing eight-member silicone rings; unfortunately, this polymer did not show much higher selectivities in the separation of $O_2/N_2$ and $CO_2/CH_4$ than other silicone polymers with similar permeabilities.[50] In light of our results, such approaches may be worthy of reconsideration by experimentalists.

## VI. Conclusion

Energetic and entropic selectivities for oxygen over nitrogen were calculated in atomic models of glassy atactic polypropylene, built following Theodorou and Suter.[20] Geometric and energetic analyses were performed on these structures with a spherical probe molecule to gain knowledge of the microstructure in the models; the locations of possible sieving constrictions, to be used as initial guesses in the transition state searches, were also located in this step. The transition-state theory method developed by Greenfield and Theodorou[11,12] was used to incorporate the polymer degrees of freedom in the simulation of the penetrant hopping process. Almost 100 diffusive hops of oxygen and nitrogen were studied in rigid as well as flexible models and rate constants were evaluated within the harmonic approximation. Subsequently the separation selectivity of each hop was partitioned into distinct energetic and entropic contributions.

Our data showed a wide range of activation barrier values; consequently, the observed rates of hopping varied over several orders of magnitude. A strong positive correlation between energetic selectivity and polymer rigidity was observed, in accordance with previous literature discussions.[2] Furthermore, our model polymer offered low entropic selectivity, in accordance with the observations of Singh and Koros.[5] However, the entropic selectivity was not correlated with rigidity of the polymer, as speculated by those authors. Rather, our data indicated that entropic selectivity is lost due to the fact the cavities in polymers tend to be smaller than those in inorganic materials, as proposed by Zimmerman and Koros.[6] The nitrogen molecule was confined more than oxygen not only in the necks but also in the cavities; thus, the entropic selectivity seen in the neck regions is offset by a comparable selectivity in the cavities. The key to improving the performance of polymer membranes seems to lie in producing larger free volume packets and not just in improving the rigidity of the necks.

We note that the results obtained in this study depend on the validity of the harmonic approximation, which is difficult to estimate. This approximation, which assumes small oscillations about a stationary point, might not be applicable in situations where the frequencies of oscillations are low, and hence the corresponding modes might explore configurations away from the stationary point of interest.[38] Hence it is desirable to calculate the rates of hopping using free energy methods, analogous to the one adopted in our previous study.[39] However, attempts in that direction require considerably more complex calculations and computational power. Efforts are currently underway in our group to implement methods to rigorously evaluate free energy barriers to penetrant hopping in polymer matrices. We also plan to study more technologically relevant polymers and state conditions.

**Acknowledgment.** The authors thank Dr. Michael L. Greenfield for many helpful discussions regarding the implementation of transition-state theory in these calculations.

## Appendix A. Form of the Model Potential

The modified LJ potential used in this work is described by the following set of equations[20]

$$U_{ij}^{LJ} = 4\epsilon_{ij}\left[\left(\frac{\sigma_{ij}}{r_{ij}}\right)^{12} - \left(\frac{\sigma_{ij}}{r_{ij}}\right)^{6}\right] \qquad r_{ij} < R_1 \tag{A1}$$

$$= \epsilon(1-\xi^3)\{A_0 + A_1\xi + A_2\xi^2\} \qquad R_1 < r_{ij} < R \tag{A2}$$

where

$$A_0 = \left.\frac{U_{ij}^{LJ}}{\epsilon}\right|_{r_{ij}=R_1} \tag{A3}$$

$$A_1 = \left.\left(3\frac{U_{ij}^{LJ}}{\epsilon} + \Delta\frac{(U_{ij}^{LJ})'}{\epsilon/\sigma}\right)\right|_{r_{ij}=R_1} \tag{A4}$$

$$A_2 = \left.\left(6\frac{U_{ij}^{LJ}}{\epsilon} + 3\Delta\frac{(U_{ij}^{LJ})'}{\epsilon/\sigma} + \frac{\Delta^2}{2}\frac{(U_{ij}^{LJ})''}{\epsilon/\sigma^2}\right)\right|_{r_{ij}=R_1} \tag{A5}$$

$$\xi = \frac{(r_{ij} - R_1)}{R} \tag{A6}$$

and

$$\Delta = \frac{(R - R_1)}{\sigma} \tag{A7}$$

The primes in the above equations denote derivatives with respect to the center-to-center distance, $r_{ij}$. $R_1 = 1.5\ \sigma_{ij}$ and $R = 2.3\ \sigma_{ij}$ are used in this study.

## References and Notes


(1) Kesting, R. E.; Fritzsche, A. K. *Polymeric Gas Separation Membranes*; John Wiley & Sons: New York, 1993.
(2) Koros, W. J.; Fleming, G. K. *J. Membr. Sci.* **1993**, *83*, 1−80.
(3) Stern, S. A. *J. Membr. Sci.* **1994**, *94*, 1−65.
(4) Robeson, L. M. *J. Membr. Sci.* **1991**, *62*, 165−185.
(5) Singh, A.; Koros, W. J. *Ind. Eng. Chem. Res.* **1996**, *35*, 1231−1234.
(6) Zimmerman, C. M.; Koros, W. J. *Macromolecules* **1999**, *32*, 3341−3346.
(7) Muller-Plathe, F. *Acta Polym.* **1994**, *45*, 259−293.
(8) Gusev, A. A.; Arizzi, S.; Suter, U. W.; Moll, D. J. *J. Chem. Phys.* **1993**, *99*, 2221−2227.
(9) Gusev, A. A.; Suter, U. W. *J. Chem. Phys.* **1993**, *99*, 2228−2234.
(10) Gusev, A. A.; Muller-Plathe, F.; van Gunsteren, W. F.; Suter, U. W. *Adv. Polym. Sci.* **1994**, *116*, 207−247.
(11) Greenfield, M. L.; Theodorou, D. N. *Mol. Simul.* **1997**, *19*, 329−361.
(12) Greenfield, M. L.; Theodorou, D. N. *Macromolecules* **1998**, *31*, 7068−7090.
(13) Chandler, D. *J. Chem. Phys.* **1978**, *68*, 2959−2970.
(14) Voter, A. F.; Doll, J. D. *J. Chem. Phys.* **1985**, *82*, 80−92.
(15) Berne, B. J.; Borkovec, M.; Straub, J. E. *J. Phys. Chem.* **1988**, *92*, 3711−3725.
(16) Hill, T. L. *An Introduction to Statistical Thermodynamics*; Dover: New York, 1986.
(17) Snurr, R. Q.; Bell, A. T.; Theodorou, D. N. *J. Phys. Chem.* **1994**, *98*, 5111−5119.
(18) Takeuchi, H. *J. Chem. Phys.* **1990**, *93*, 2062−2067.
(19) Vineyard, G. H. *J. Phys. Chem. Solids* **1957**, *3*, 121−127.
(20) Theodorou, D. N.; Suter, U. W. *Macromolecules* **1985**, *18*, 1467−1478.
(21) van Gunsteren, W. F.; Karplus, M. *Macromolecules* **1982**, *15*, 1528−1544.
(22) *MSI. Cerius2 User Guide*, March 1997 ed.; Molecular Simulations Inc.: San Diego, CA, 1997.
(23) Flory, P. J. *Statistical Mechanics of Chain Molecules*; Wiley: New York, 1969.
(24) Goldstein, H. *Classical Mechanics*; Addison-Wesley: Reading, MA, 1950.
(25) Byrd, R. H.; Lu, P.; Nocedal, J.; Zhu, C. *SIAM J. Sci. Comput.* **1995**, *16*, 1190−1208.
(26) Allen, M. P.; Tildesley, D. J. *Computer Simulation of Liquids*; Clarendon Press: Oxford, England, 1987.
(27) Arizzi, S.; Mott, P. H.; Suter, U. W. *J. Polym. Sci., Polym. Phys. Ed.* **1992**, *30*, 415−426.
(28) Greenfield, M. L.; Theodorou, D. N. *Macromolecules* **1993**, *26*, 5461−5472.
(29) Misra, S.; Mattice, W. L. *Macromolecules* **1993**, *26*, 7274−7281.
(30) Gusev, A. A.; Suter, U. W. *Phys. Rev. A* **1991**, *43*, 6488−6494.
(31) June, R. L.; Bell, A. T.; Theodorou, D. N. *J. Phys. Chem.* **1991**, *95*, 8866−8878.
(32) Cerjan, C. J.; Miller, W. H. *J. Chem. Phys.* **1981**, *75*, 2800−2806.
(33) Baker, J. *J. Comput. Chem.* **1986**, *7*, 385−395.
(34) Wales, D. J. *Mol. Phys.* **1991**, *74*, 1−25.
(35) Wales, D. J. *J. Chem. Phys.* **1994**, *101*, 3750−3762.
(36) Fukui, K. *Acc. Chem. Res.* **1981**, *14*, 363−368.
(37) Banerjee, A.; Adams, N. P. *Int. J. Quantum Chem.* **1992**, *43*, 855−871.
(38) Greenfield, M. L. Molecular Modeling of Dilute Penetrant Gas Diffusion in a Glassy Polymer using Multidimensional Transition-State Theory. Ph.D. Thesis, University of California at Berkeley, 1996.
(39) Rallabandi, P. S.; Ford, D. M. *AIChE J.* **2000**, *46*, 99−109.
(40) Voter, A. F. *J. Chem. Phys.* **1985**, *82*, 1890−1899.
(41) Karger, J.; Ruthven, D. M. *Diffusion in Zeolites and Other Microporous Solids*; John Wiley & Sons: New York, 1992.
(42) Shantarovich, V. P.; Azamatova, Z. K.; Novikov, Y. A.; Yampolskii, Y. P. *Macromolecules* **1998**, *31*, 3969−3966.
(43) Yu, Z.; McGervey, J. D.; Jamieson, A. M.; Simha, R. *Macromolecules* **1995**, *28*, 6268−6272.
(44) Shah, V. M.; Stern, S. A.; Ludovice, P. J. *Macromolecules* **1989**, *22*, 4660−4662.
(45) Rigby, D.; Roe, R. J. *Macromolecules* **1990**, *23*, 5312−5319.
(46) Trohalaki, S.; DeBolt, L. C.; Mark, J. E.; Frisch, H. L. *Macromolecules* **1990**, *23*, 813−816.
(47) Boyd, R. H.; Pant, P. V. K. *Macromolecules* **1991**, *24*, 6325−6331.
(48) Bharadwaj, R. K.; Boyd, R. H. *Polymer* **1999**, *40*, 4229−4236.
(49) Zhang, X.-S. Ph.D. Dissertation, Academia Sinica at Beijing, 1987.
(50) Mi, Y.; Stern, S. A. *J. Polym. Sci., Part B: Polym. Phys.* **1991**, *29*, 389−393.
(51) Fischer, J.; Lago, S. *J. Chem. Phys.* **1983**, *78*, 5750−5758.


MA991599U